Eurasian Journal of Physics and Functional Materials

Volume 6 | Number 1

Article 2

Pages: 18 - 31

3-22-2022

Flexible algorithms for background suppression in heavy ion induced nuclear reactions

D. Ibadullayev

Yu. S. Tsyganov

A. N. Polyakov

A. A. Voinov

V. G. Subbotin

See next page for additional authors

Recommended Citation

Ibadullayev, D.; Tsyganov, Yu. S.; Polyakov, A. N.; Voinov, A. A.; Subbotin, V. G.; and Shumeiko, M. V. (2022) "Flexible algorithms for background suppression in heavy ion induced nuclear reactions," *Eurasian Journal of Physics and Functional Materials*: Vol. 6: No. 1, Article 2.
DOI: https://doi.org/10.32523/ejpfm.2022060102

Flexible algorithms for background suppression in heavy ion induced nuclear reactions

Authors

D. Ibadullayev, Yu. S. Tsyganov, A. N. Polyakov, A. A. Voinov, V. G. Subbotin, and M. V. Shumeiko

Eurasian Journal of Physics and Functional Materials

2022, 6(1), 18-31

Flexible algorithms for background suppression in heavy ion induced nuclear reactions

D. Ibadullayev*[1,2], Yu.S. Tsyganov[1], A.N. Polyakov[1], A.A. Voinov[1], V.G. Subbotin[1], M.V. Shumeiko[1], L. Schlattauer[3]

[1]Joint institute for nuclear research, Dubna, Russia

[2]The Institute of Nuclear Research, Almaty, Kazakhstan

[3]Palacky University, Olomous, Czech Republic

E-mail: Ibadullayev@jinr.ru

DOI: **10.32523/ejpfm.2022060102**
Received: 17.03.2022 - after revision

A new algorithm for the analog spectrometer of the DGFRS-2 setup installed at DC-280 cyclotron is presented. The main goal of application of this algorithm is to search an optimal time correlation recoil-alpha parameter directly during the acquisition C++ code execution. A new real-time flexible algorithm in addition to the conventional $ER - \alpha$ algorithm, which has been used for a several years at the DGFRS-1 setup installed at the U-400 FLNR cyclotron, is presented. The main parts of the spectrometer are a 48×128 strip DSSD detector (Double Side Strip Detector) and a low-pressure gaseous detector. They are presented schematically. Nuclear reactions for synthesis of element Z=119 at the DGFRS-2 are under consideration. Some attention is paid to computer simulation of the heavy recoil spectra, taking into account its pulse height defect in silicon. First beam test results are also presented. A new formula for half-life time using recent data for superheavy nuclei is obtained.

Keywords: superheavy elements; correlation; strip detector; analog spectrometer; separator; cyclotron; evaporation residue

Introduction

With the discovery of uranium fission by Hann and Strassmann, the nuclei existence boundary was physically defined for the first time as a limit of nuclei

stability with the spontaneous fission (SF) [1]. The fission barrier will promptly decrease with growing Z (Z > 92) [2]. In the macroscopic theory the situation with zero barrier occurs for the element with Z > 100. The situation is changed after observing the short spontaneous fission half-life of ^{242}Am (TSF $\approx$ 0.014 s), which has T_{SF} > 3e+12 y in the ground state [3]. It means that nuclear structure does not disappear with increasing deformation but evolves an important role in nuclear fission process [4]. Elements with Z > 100 were produced in the reactions induced by charged particles.

In the beginning of present century, new Z = 114-118 elements were synthesized using the Dubna Gas-Filled Recoil Separator (DGFRS) [5-10]. That discovery confirmed the main role of shell effects in stability of superheavy nuclei. From the viewpoint of detecting procedure, the specifics of that experiment are in detection of ultra-rare α-decays or/and SF signals. A key issue is the probability P_{err} that the observed sequence of event is due to a random correlation of unrelated events. The value of this probability allows readers and experimenters to judge the reliability of the interpretation. Present work aimed to a development of flexible real-time algorithms to decrease significantly P_{err} parameter, and, therefore, to provide a higher interpretation validity.

Experimental technique

To synthesize new superheavy nuclei, the following technique should be in operation:

• Ion source and accelerator to provide high projectile intensity because of extremely low cross-section values of the products under investigation formation;

• Rotating actinide target: its design should provide long-term non-destructive operation under condition of high intensity of heavy ion beams;

• Recoil separator: it should provide a high level of background products suppression and relatively high transmission factor for the products under investigation;

• The detection system: High separation yield will increase background level, so the transmitted particles must be identified by detector system with high efficiency. During the last 30 years, these DGFRS-1 silicon detectors have been transformed from surface-barrier detectors based on n-Si(Au) into resistive layer PIPS position sensitive ones, and then into DSSD detectors. Namely, DSSD large area detectors are mostly efficient for ultra-rare α-decays detection.

The new detector system is composed of low-pressure (1.2 $\pm$ 0.0017 Torr pentane) proportional chamber detector and 48×128 strips DSSD focal plane detector, 8 strips 6 backward detectors, VETO-detector [11, 12]. Figure 1 shows the schematic of the detector module. The thickness of the entrance Mylar foil is about 1.2 μm. A silicon-veto detector to suppress the background particles passing through the DSSD focal plane completes the setup. The additional electrode, shown in Figure 1, located at a distance of 6 cm apart from ΔE detector in the direction of DSSD one, is based by -200 V to reduce an influence of space charge to the parameter of detection efficiency under condition of high rate of

highly ionized charged particles passing through ΔE detector (up to $\sim$1e+4 s^{-1}).

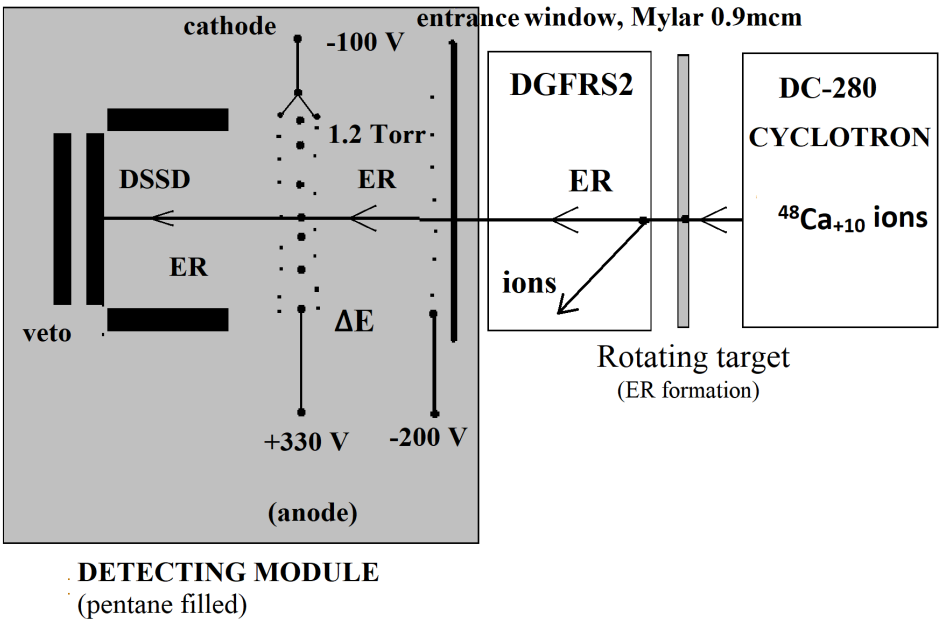

Figure 1. Schematics of the detecting module of the DGFRS-2 setup.

Although a detailed description of the electronics is beyond the scope of the author, in order to help the reader understand the whole data taking process, Figure 2 shows general block schematics of the DGFRS-2 spectrometer. The main electronic modules with their functions are presented in the Table 1.

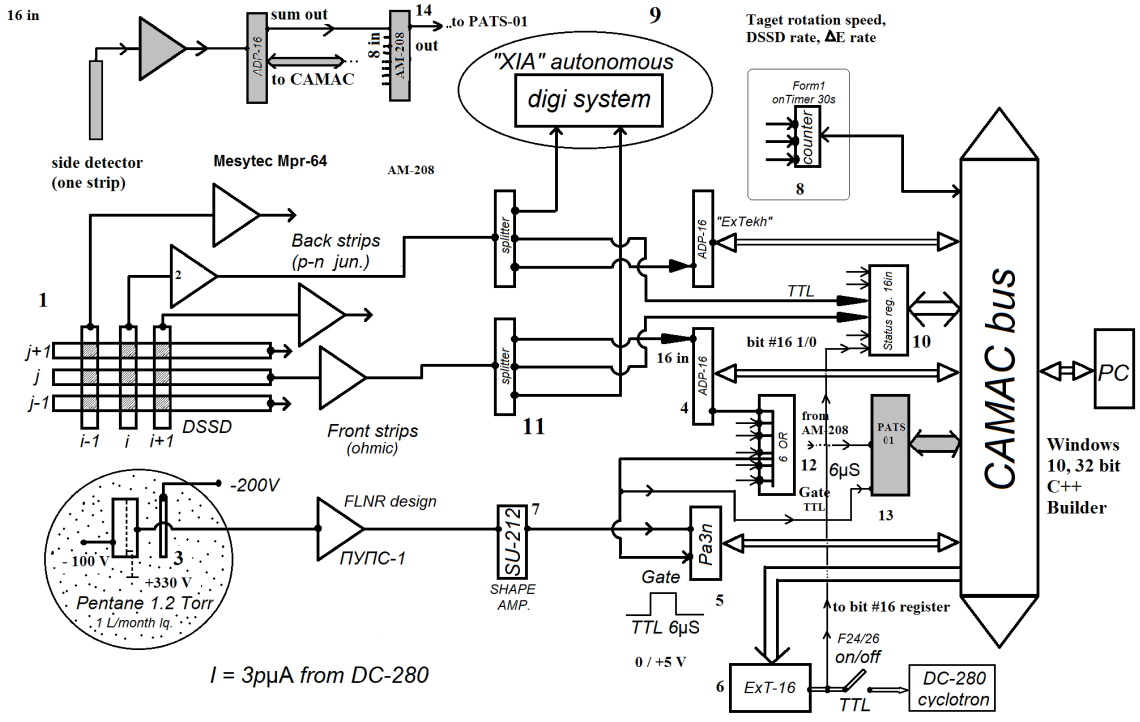

Figure 2. Schematics of the analog spectrometer for real-time search for short ER-α correlated sequences. The branch corresponding to one strip of side detector is shown in gray.

Table 1.
Main electronic units of the analog spectrometer.

Number on Figure 2	Unit name	Function (in brief)
1	Double Side Silicon Strip Detector	To measure ER, α, SF and other signals.
2	Mesytec Mpr-64	Charge sensitive preamplifier.
3	ΔE low pressure pentane filled proportional chamber	To measure signal from charged particle coming from cyclotron DC-280.
4	Analog processor ADP-16 1M	16-in, two scales shaping amplifier-analog multiplexer-analog to digital converter: 13 bit first scale(<27 Mev), 12 bit second scale (< 270 Mev).
5	Pa3n	3-in 1M unit to measure ΔE signals. 12 bit/channel.
6	Ext-16	2M unit to create "STOP" TTL signal to stop irradiation process.
7	SU-212 2M	Shaping amplifier (FLNR, JINR design) to measure ΔE signals.
8	16 bit counter	1M unit to measure target rotation speed, event rate of DSSD.
9	XIA digital system	XIA Corporation digital spectrometer (autonomous).
10	Status 16 bit register	Start read-out process if are there any non-zero signals of "L" any ADP of front strips (48 strips).
11	Splitter unit 3M	32-in unit to split signals from preamplifiers to digital and analog system(FLNR, JINR design).
12	1M unit 6OR	6-in logical TTL input signals to provide trigger TTL signal for gating of Pa3n unit.
13	1M unit PATS01	12 bit ADC to measure summary signal from all side detectors (FLNR, JINR design).
14	1M unit AM-208	8- in analog multiplexer(FLNR, JINR design).

The DGFRS-2 spectrometer consists of two independent branches. One is a digital spectrometer based on PIXIE-16 modules produced by XIA Corporation [13]. This subsystem allows detecting very short events with $\sim$120 ns dead time, whereas the second one based on ADP-16 CAMAC (manufacturer "ExTekh" firm, free economy zone "Dubna") units and allows detecting sequences of eight events with 2.8 μs time interval between each two signals [14]. Regular dead time of analog branch is about 25 μs. Searching for the ER-α correlation

is performed with the second subsystem. Of course, it is assumed that 482 calibration parameters are ready for application before the starting the experiment. To obtain the calibration parameters, we usually use heavy ion induced complete fusion nuclear reaction ^{nat}Yb+^{48}Ca$\rightarrow$ ^{217}Th+3n and some others (xn) reactions of similar nature [11, 12].

Method of active correlations

The heaviest element 118 (Og) was observed by a heavy ion induced complete fusion nuclear reaction, namely in ^{249}Cf+^{48}Ca$\rightarrow$Og*. A first successful experiment to synthesize Z=118 element was made at DGFRS-1 in 2003, using a net irradiation time of 60 days and a beam dose of $4.3\cdot10^{18}$ [15]. The experiment was continued in 2006, reaching net irradiation time 4 months and beam dose of $4.1\cdot10^{19}$ [16]. As a result, four decay chains of ^{294}Og were observed. Note, that previous experiment to synthesize Z=118 element was strongly unsuccessful [16]. As to the synthesis of Z = 120 element, the experiment ^{244}Pu+^{58}Fe$\rightarrow$120* was unsuccessful too [17]. Only upper limit of cross-section value of 0.8 pb has been declared. With putting into operation both ultra-intense new FLNR cyclotron DC-280 and DGFRS-2 setup, we plan to synthesize new elements Z=119, 120. The most reasonable candidates to working reactions are: ^{243}Am + ^{54}Cr $\rightarrow$ ^{294}119 + 3n, ^{249}Bk + ^{50}Ti $\rightarrow$ 119 + 3n, ^{244,242}Pu + ^{58}Fe $\rightarrow$ ^{302,300}120 + 3n, ^{249}Cf + ^{50}Ti $\rightarrow$ ^{296}120 + 3n. The significant role in the discoveries of Z=113-118 elements played method of "active correlations". Namely, these techniques one can definitely consider as a "locomotive" which provides background free detection procedure for alpha decays of super heavy nuclei under investigation. Moreover, with an increasing of beam intensity, significance of this method will also increase. To apply this method correctly, one should predict energy-time property of nuclei under investigation with some accuracy. In the Table 2 (3^{rd} and 4^{th} column) $Q\alpha - T\alpha$ parameters of SHN measured in ^{48}Ca induced complete fusion reactions performed at the DGFRS-1 setup are presented basing on the Table 1 from the Ref. [5]. The column 5 with calculated values of T_{α}^{calc} corresponds to the formulae [18]:

$$T_{\alpha}^{calc} = 10^{(aZ+b)\cdot Q^{-1/2}+c\cdot Z+d} \quad (1)$$

where a=1.78, b=-21.398, c=-0.25488 and d=-28.423 [19]. The K-parameter which was whown in Figures 3 is equal to $K = T_{\alpha}^{calc}/T_{\alpha}$. In the Figure 3a, b dependence of LgK against Z value is shown. Figure 3b corresponds to an improved calculation with d=-28.0928 (last column). This d value is obtained via iteration process with condition $|\,\mathrm{mean}_i\,| < 10^3$, where i – index of iteration process. For the sake of comparison, several T_{α} values calculated using Royer's formulae are presented in the last column 6, lgK values are shown in Figure 3c. In contrast to formulae (1) containing two parameters (Q_{α}, Z) Royer's formulae contain three parameters, namely Q_{α}, Z and A [20].

Table 2.
Alpha decay properties of the superheavy nuclei.

Z	A	Q_α [MeV]	T_α [ms]	T_α^{calc} [ms]	T_α^{Royer} [ms]	T_α^{calc2} [ms]
118	294	11.82	0.69	0.415	0.144	0.89
117	294	11.18	51	7.84	26.3	16.77
117	293	11.32	22	3.52	11.8	7.52
116	293	10.71	57	66.3		141.85
116	292	10.78	13	22.4	30	47.9
116	291	10.89	19	11.69		25
116	290	11.00	8.3	216.5		462.99
115	290	10.41	650	131.0	2000	280.25
115	289	10.49	330	55.2		118.01
115	288	10.63	164	26.6	184	56.99
115	287	10.75	37	1741.8	246	3725.69
114	289	9.98	1900	960.5		2054.43
114	288	10.07	660	500.4	593	1070.26
114	287	10.17	480	158.5		338.92
114	286	10.35	120	3034.6	108	6490.86
113	286	9.79	9500	698.9		1495
113	285	10.01	4200	341.5	6050	730.53
113	284	10.12	910	65.8		140.7
113	283	10.38	75	5.87	41	12.55
113	282	10.78	73	38789.1		82967.91
112	285	9.32	28000	3539.6		7570.95
112	283	9.66	4200	3540		43.24
112	281	10.46	100	20.2		123733.69
111	282	9.16	100000	57847.9		20439.3
111	281	9.41	17000	9555.8		2.22
111	278	10.85	4.2	1.04		2.4
110	277	10.72	6	1.1		1416.38
109	278	9.58	4500	662.2	1430	0.89

Another required step for active correlations' method application is an exhaustive knowledge about registered amplitude values of implanted heavy nuclei. There are two approaches to that task, one of them is to use the empirical dependence of the registered energy on the incoming calculated energy using reactions leading to the complete fusion products close to Z=100 with relatively high cross-sections [20]. Another approach is related to computer simulation of heavy recoil registered energy spectra [21]. The code described in Ref. [21] allows a simulation that considers the reasons for transformation of spectra originating in the target into that registered by a silicon detector. In the Fig.4 both measured in ^{242}Pu+^{48}Ca$\rightarrow$Fl* reaction and simulated spectra are shown. The arrows show the registered recoil amplitudes measured in ^{238}U+^{48}Ca$\rightarrow$ ^{283}Cn+3n experiment. They demonstrate a perfect correspondence to each other.

The synthesis superheavy elements Z = 119, Z = 120 using the heaviest

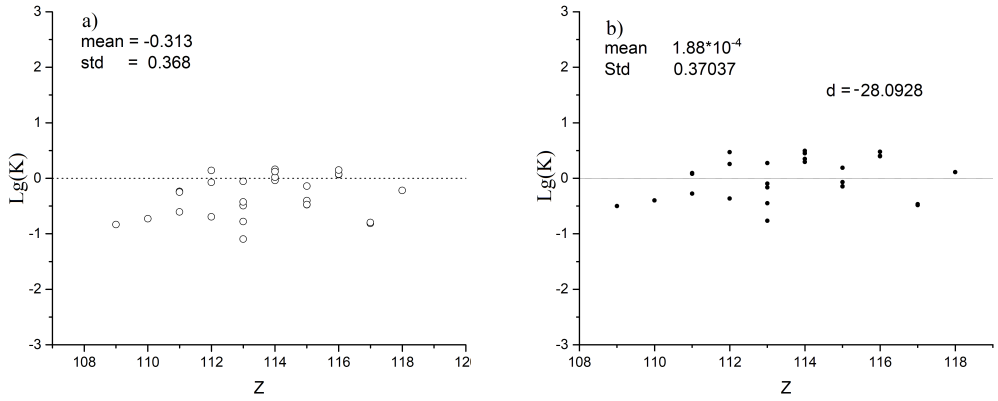

Figure 3. Dependence of $Lg(K)$ value against Z for isotopes of nuclei Z = 109-118 (a: d = -28.423, Ref. [18]; b: d = -28.0928).

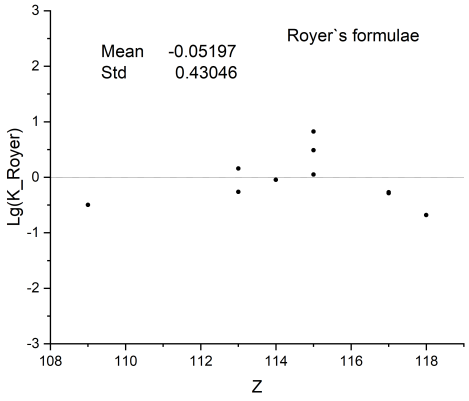

Figure 3c. Dependence of $Lg(K)$ value against Z for isotopes of nuclei Z = 109-118 with Royer's formulae.

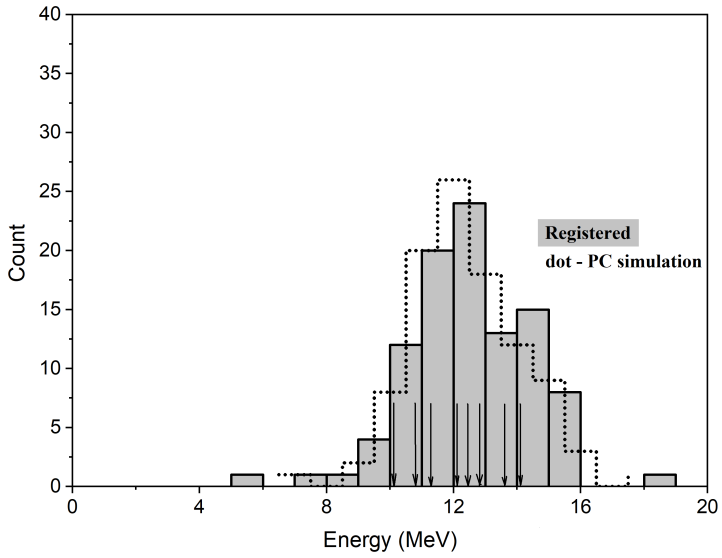

Figure 4. Registered and computer simulated (dot line) spectra of implanted recoils from ^{242} Pu+ ^{48} Ca → Fl* complete fusion reaction. Arrows show recoil nuclei of ^{283} Cn registered in ^{238} U + ^{48} Ca reaction.

available target materials ^{249}Bk, ^{251}Cf requires to switch to the higher-Z bombarding particles ^{50}Ti, ^{54}Cr except for double magic projectile ^{48}Ca. However, the cross-sections of fusion reactions with heavier projectiles are expected to be significantly lower than with ^{48}Ca. Therefore, it is necessary to increase noticeable the overall experiment efficiency. To solve this problem a new experimental complex is developed at FLNR (JINR) including the specialized high-current DC-280 cyclotron and new DGFRS-2 gas-filled recoil separator [22]. Of course, with higher beam intensity, requirement to suppress background products when detecting ultra-rare α-decays is of great significance. Below, in the Table 3, the predicted decay chains of ^{294}119 nuclei are shown [18, 23]. $T_{1/2}$ and Q_α of the isotopes 105-117 measured in the experiments on DGFRS-II [5].

Table 3.
Alpha decay properties of the superheavy nuclei.

Z	A	Q_α [MeV]	$T_{1/2}$ [ms]	sourse
119	294	12.338	0.11	[see Figure 25 from Ref. 23,18] *d*= -28.0928
117	290	11.74	3.14	[5, 18]
115	286	10.87	34.5	[5, 18]
113	282	10.78	73	[5]
111	278	10.85	4.2	[5]
109	274	10.2	440	[5]
107	270	9.06	61000	[5]
105	266	Spontaneous fission	1 320 000	[5]

Choice of initial parameters for "active correlations" technique application

Below, we shall consider different detection modes of an "active correlations" method, which are based on:

- Standard algorithm;
- Simple-flexible algorithm (trivial);
- Flexible-probability algorithm;
- High recoil signals rate algorithm;
- Combined algorithm.

Standard algorithm

This approach is applied at both DGFRS-2 and DGFRS-1 during last year's (see e.g. [24]). The correlation time parameter is chosen from the upper presented $T_\alpha = f(Q_\alpha)$ systematic as $T_{corr} = n \cdot T_\alpha$, where $n \gg 1$.

As usual, it uses a fixed $ER - \alpha$ correlation time interval, pre-setting by the experimentalist. In some cases, a functional dependence $t = F(E_\alpha)$.

Here E_α is the current value of the energy signal of alpha particle (or even imitating the alpha decay signal) and relation from [18] defines function F. In the Figure 5, such dependence is shown for different beam intensities for DGFRS-1 setup installed at U-400 cyclotron of FLNR.

Typical correlation time parameters are usually taken from1 to 5 s, with beam pause times of 1 to 2 minutes for those experiments.

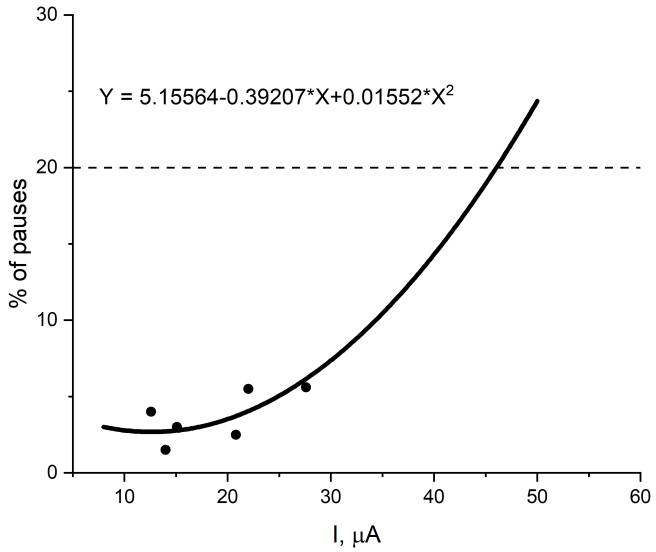

Figure 5. Typical target irradiation whole time losses against the beam intensity at the DGFRS-1 setup at a correlation time of 1 s and a pause time of 1 min ($^{48}Ca^{+18}$). The dotted line shows the 20% level.

Note, that the background suppression factor for the DGFRS-2 is much greater than for the DGFRS-1 setup [23]. Thus, irradiation time losses are much smaller in the similar experiments (^{48}Ca + Actinide target $\rightarrow$ *SHN). For instance, in the reaction ^{242}Pu + ^{48}Ca $\rightarrow$ ^{287}Fl + 3n typical rate of random correlation beam stops value was about one-two per day at the DGFRS-2. It means when one takes into account the correlation time parameter 20 s and pause time 100 s, beam time loss will be about $\sim$400 s per day, or $\sim$0.5% from the whole irradiation time. An average $^{48}Ca^{+10}$ beam intensity was about 3 pμA from DC-280 cyclotron. In the $^{238}\mathrm{U} + ^{48}\mathrm{Ca} \rightarrow ^{283}\mathrm{Cn} + 3n$ complete fusion reaction, the projectile beam intensity was up to $\sim$7 pμA for a few days.

Simple - flexible (trivial) algorithm

In this scenario, after the experimenter boots code, the first approximation for the $ER - \alpha$ correlation parameter Tcorr is read from the appropriate text file.

Each time interval (event onTimer C++ Builder) of 5-10 min, the code adds one T_{corr} value until the iteration number is less than N_{max} or the beam stop is already occur.

Here, N_{max} - is a pre-set integer parameter (usually $\sim$10 or even more).

Flexible - probability algorithm (main)

The application of this algorithm was tested on the DC-280 ^{48}Ca beam in various nuclear reactions. In our experiments, we apply a specific acquisition mode. Namely, when energy-time-position correlation like $ER - \alpha$ is detected, the system switches the beam off for a short time. Therefore, the forthcoming decay signals are detected in a background free mode. For example, if we start acquisition Builder C++ program with initial conditions as:

- T_{corr} is a first approximation of the correlation $ER - \alpha$ time value;
- Δ t - beam stop pause time(fixed, usually 100-300 s);
- N_{b0} - random correlation expectation for one day acceptable by the experimentalists (float).

After booting, the new file system estimates each ten minutes an actual expectation value with the extrapolation to 24 hours using mean ER and α signals rate value and corrects T_{corr} parameter. When T_{corr}^{k} corresponds to the condition $\mid N_b^k - N_{b_0} \mid < \varepsilon$, where ε is a small positive value ($\varepsilon \ll 1$), system stops iteration process. In the Figure 6 an example of the mentioned algorithm application is shown for one decay chain of ^{288}Mc isotope that was registered in $^{243}Am + ^{48}Ca \rightarrow Mc*$ complete fusion reaction. This experiment was carried out at the DGFRS-2 installation of the Superheavy Element Factory. During the experiment, 61 decay chains of two Mc isotopes were registered. Daughter nuclei which shown with shadows was registered after finding the ER-α correlation, during beam off time. To a first approximation, τ_0 value was equal to 1 s and $N_{b0} = 4$.

The iteration process flows in the form: $T_k = T_{k-1} \cdot N_{b0} / N_b^{k-1}$, where k is a number of iteration.

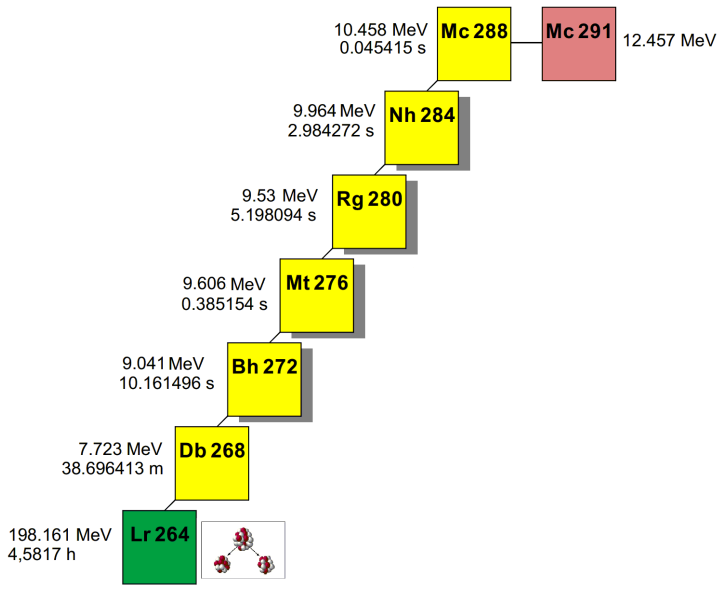

Figure 6. Decay chain of ^{291} Mc nucleus implanted into DSSD detector. Shadows indicate to the signals are within a beam off time interval.

Additional successful test of the described algorithm application was performed in ^{242}Pu + ^{48}Ca $\rightarrow$ *Fl complete fusion nuclear reaction with up to 3 pμA projectile beam intensity for a few hours. Below, in the Figure 7 duration of the iteration process is shown as example. Note, that system stops iteration process for 70 minutes.

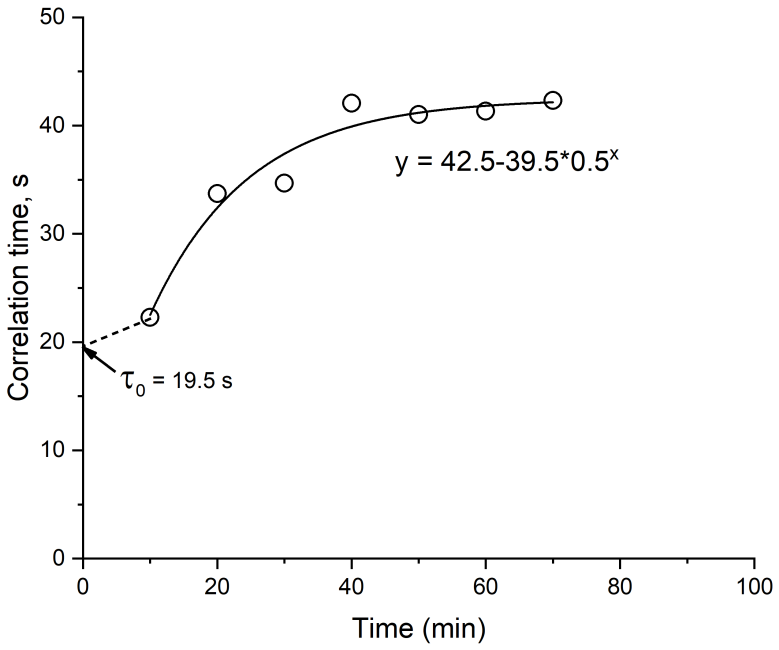

Figure 7. Flexible algorithm iteration (Builder C++ *onTimer* event) process in ^{242}Pu + ^{48}Ca $\rightarrow$ *Fl reaction. Line shows exponential fit.

Note, that during the calculation the probability of each ER-α correlation chain to be a random, calculation operates with the parameter of effective area A_{eff}. The algorithm to calculate that parameter is presented below using coding in Python [25].The process of recalculation is usually performed for every 20-30 min.

The algorithm is designed to calculate the effective area of the focal plane detector - that is, the percentage of the detector area, which is 0.95 of the total dose (see Figure 8). Initially, the Levenberg-Marquardt gradient descent algorithm is used, but it showed low accuracy due to the complex relief of the dose distribution [26]. The algorithm entered the wrong local minimum and showed an incorrect estimation. The new algorithm can be illustrated as filling a vessel with an uneven bottom with water drops. As the filling is completed, the accumulated dose is calculated and checked for compliance with the factor.

High ER signal rate algorithm

The authors do not exclude the possibility that heavy-ion projectile intensity at the DC-280 FLNR cyclotron will reach such a high level, as the ER's rate will be high enough to start iteration process leading to a smaller parameter of T_{corr} than the

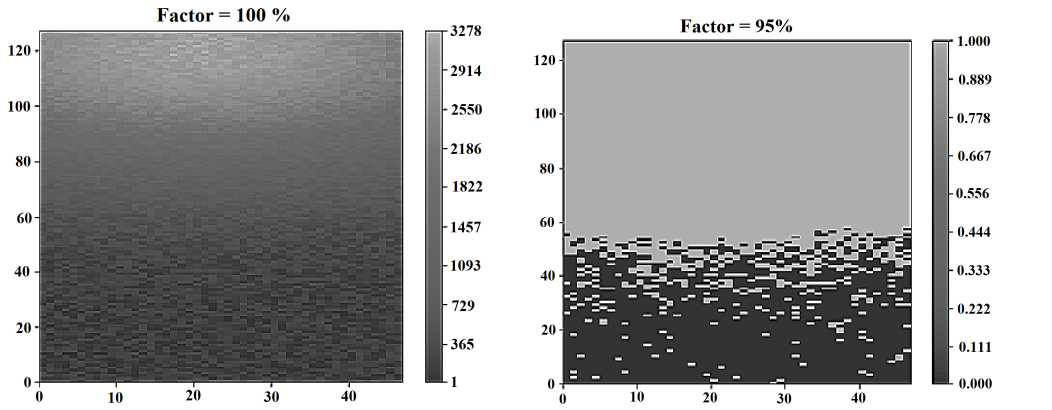

Figure 8. Left figure: The result of the algorithm - light marks all cells on the area of which a dose equal to factor = 1.0 is distributed. Right figure: The same as in the left figure, but for dose equal to factor 0.95. A_{eff} = 0.63.

first approximation one. In this case, the acquisition program changes the trigger signal sequence. Namely, except for ER-α sequence it will consider ER-$\alpha - \alpha$ energy-time-position correlation and, therefore, will use a more sophisticated algorithm. This approach was not tested at the DC-280 beam until now, but it was tested using a Monte Carlo PC-based simulation reported in [21]. The preliminary general conclusion of those simulations show that there is no need to switch the algorithms in the range from 1 to 10 pμA of the ^{48}Ca beam.

In the nearest future, we plan to extend similar conclusion for another projectiles, like ^{50}Ti and ^{54}Cr.

Combined algorithm

In principle, the same as flexible algorithm, but, additionally the range for the ER signal (left level) is varied by a small amount of ± 1 MeV with an iteration step of 0.2 MeV. In addition, the beam off pause time interval is varied for a small value, usually of $\pm 15\,\%$ with respect to a first assignment one too.

Conclusion

With the commissioning of the new super intense FLNR DC-280 heavy ion cyclotron and the new DGFRS-2 setup, new approach to the real-time algorithm for a radical suppression of background signals in heavy ion induced complete fusion reactions has been designed basing on a flexible scenario for a choice of the value of time correlation ER-α interval. First tests were successfully carried out with an intense ^{48}Ca beam up to several pμA are successfully performed. The design of the DGFRS-2 setup allowed using those time intervals up to tens of seconds, even at a ^{48}Ca intensity up to 3-5 pμA. We plan to apply a similar algorithm in the forthcoming experiments with ^{54}Cr and ^{50}Ti projectiles aimed to the synthesis of Z=119 element in the nearest future. In addition, we will try to develop a similar algorithm and appropriate software for digital electronics

manufactured by XIA Corporation. The first approximation of the time interval value following from the presented $Log(T_\alpha) = (aZ + b) \cdot Q^{-1/2} + c \cdot Z + d$ with d = -28.0928 formula, can be considered as a quite satisfactory. The spectrum of the ER registered energy for ^{54}Cr + ^{238}U $\rightarrow$ ^{289}Lv + 3n complete fusion nuclear reaction has been calculated. The estimated half-life value for ^{294}119 nuclei of about $\sim$110 μs will definitely allow applying the described analog spectrometer to detect such ER-α correlated sequence.

One general extra conclusion can be drawn here, namely, development of the whole detection system (not only algorithms, software) including extensive beam tests is in progress now.

Acknowledgments

This paper is supported in part by the Ministry of Science and Higher Education of the Russian Federation through grant No. 075-10-2020-117

References

[1] O. Hahn et al., Naturwissenschaften **27** (1939) 11. [*CrossRef*] (In German)
[2] L. Meitner et al., Nature **143** (1939) 239-240. [*CrossRef*]
[3] S.M. Polikanov et al., Zh. Exp. Theor. Phys. **42** (1962) 1464.
[4] V.M. Strutinsky et al., Nucl. Phys. A **95** (1967) 420. [*CrossRef*]
[5] Yu.Ts. Oganessian, V.K. Utyonkov, Nucl. Phys. A **944** (2015) 62-98. [*CrossRef*]
[6] Yu.Ts. Oganessian, V.K. Utyonkov, Rep. Prog. Phys. **78** (2015) 034301. [*CrossRef*]
[7] Yu.Ts. Oganessian et al., Phys. Rev. C **87** (2013) 034605. [*CrossRef*]
[8] Yu.Ts. Oganessian et al., Phys. Rev. Lett **108** (2012) 022502. [*CrossRef*]
[9] Yu.Ts. Oganessian et al., Phys. Rev. C **74** (2006) 044602. [*CrossRef*]
[10] Yu.Ts. Oganessian et al., Phys. Rev. C **83** (2011) 054315. [*CrossRef*]
[11] Yu.S. Tsyganov, D. Ibadullayev et al., Acta Phys. Polonica B **14** (2021) 767-774. [*CrossRef*]
[12] D. Ibadullayev, Yu.S. Tsyganov et al., Acta Phys. Polonica B **14** (2021) 873-878. [*CrossRef*]
[13] 31057 Genstar Rd, Hayward, CA 94544 USA, "Pixie-16 User Manual". XIA LLC, v.03 (2019) 92. [*WebLink*]
[14] Yu.S. Tsyganov et al., Phys. of Part. and Nuclei Lett. **13** (2016) 112-119. [*CrossRef*]
[15] Yu.Ts. Oganessian et al., LLNL UCRL-ID-151619 (Livermore 2003) [*CrossRef*]
[16] V. Ninov et al., Phys. Rev. Lett. **83** (1999) 1104. [*CrossRef*]
[17] Yu.Ts. Oganessian et al., Phys. Rev. C **79** (2009) 024603. [*CrossRef*]
[18] Yu.S. Tsyganov et al., Nucl. Instrum. And Meth. In Phys. Res. A **558** (2006) 329-332. [*CrossRef*]
[19] Zhishuai Ge et al., Phys. Rev. C **98** (2018) 034312. [*CrossRef*]
[20] Yu.S. Tsyganov et al., Phys. of Part. and Nuclei Lett. **49** (2018) 1036-1045. [*CrossRef*]

[21] Yu.S. Tsyganov et al., Nucl. Instrum. And Meth. In Phys. Res. A **378** (1996) 356-359. [*CrossRef*]
[22] Yu.Ts. Oganessian et al., Submitted to Nucl. Instrum. and Meth. B (2022)
[23] M. Wang et. al., Chin. Phys. C **36** (2012) 1603-2014. [*CrossRef*]
[24] Yu.S. Tsyganov et al., Nucl. Instrum. And Meth. In Phys. Res. A **525** (2004) 213-216. [*CrossRef*]
[25] L. Ramallo, Fluent Python, O'Reilly Media, Inc. (2015) 1390. [*WebLink*]
[26] K. Levenberg et al., J. Quart. Appl. Math. **2** (1944) 164-168. [*CrossRef*]